AJRCCM Articles in Press. Published on 08-February-2018 as 10.1164/rccm.201708-1728OC

Unstable Inflation Causing Injury: Insight from Prone Position and Paired CT Scans

Yi Xin[1*], Maurizio Cereda[2*], Hooman Hamedani[1], Mehrdad Pourfathi[1], Sarmad Siddiqui[1], Natalie Meeder[2], Stephen Kadlecek[1], Ian Duncan[1], Harrilla Profka[1], Jennia Rajaei[3], Nicholas J. Tustison[4], James C. Gee[1], Brian P. Kavanagh[5], Rahim R. Rizi[1]

[1]Department of Radiology, University of Pennsylvania, Philadelphia, PA, USA; [2]Department of Anesthesiology and Critical Care, University of Pennsylvania, Philadelphia, PA, USA; [3]Stanford University, Stanford, CA, USA; [4]Department of Radiology and Medical Imaging, University of Virginia, Charlottesville, VA, USA; [5]Departments of Critical Care Medicine and Anesthesia, Hospital for Sick Children, University of Toronto, Canada

** Yi Xin and Maurizio Cereda share lead authorship role in this work.*

Corresponding Author: Rahim R. Rizi, Professor of Radiology, University of Pennsylvania, 3400 Spruce Street, MRI Learning Center, Philadelphia, PA, 19104, Tel: 215-615-2426, Email: rizi@uphs.upenn.edu

Author Contributions: Y.X., M.C., B.K. and R.R. study conception and design; Y.X., M.C., N.M., and H.P. acquisition of data; Y.X., M.C., H.H., M.P., S.S., N.M., S.K., N.T., J.G., B.K. and R.R. analysis and interpretation of data; Y.X., M.C., I.D., J.R., J.G. and B.K. drafting of manuscript; Y.X., M.C., H.H., S.K., I.D., J.G., B.K., R.R. critical revision.

Funding: This work was supported by NIH (Bethesda, MD, USA) grants R01-HL139066 and R01-HL124986. Maurizio Cereda was supported by a grant from the Foundation for Anesthesia Education and Research (Schaumburg, IL) and from the Society of Critical Care Anesthesiologists (Park Ridge, IL, USA), and by the Transdisciplinary Awards Program in Translational Medicine and Therapeutics (Philadelphia, PA). Brian P. Kavanagh is supported by operating funds from the CIHR (Ottawa, ON, Canada) and holds the Dr. Geoffrey Barker Chair in Critical Care Medicine.

Running Head: Prone position reduces injury by stabilizing inflation

Subject Category: 4.8 Mechanical Ventilation: Physiology & Pathophysiology

Word Count: 3298

This article has an online data supplement, which is accessible from this issue's table of content online at www.atsjournals.org

AT A GLANCE COMMENTARY

Scientific Knowledge on the Subject: Ventilation in the prone position increases oxygenation and improves survival in severe acute respiratory distress syndrome (ARDS); however, the specific mechanism through which prone positioning improves survival is not known.

What This Study Adds to the Field: Using paired, serial CT scans taken at inspiration and at expiration, we identified regions of unstable inflation –partially aerated voxels with large tidal swings in tissue density– that indicate local lung stress. We report that prone positioning contains the early propagation of ventilator-associated lung injury, an effect that is related to reduced vertical gradients of unstable inflation. This imaging approach may ultimately improve clinical prognostication by identifying patients with ARDS who have a higher (or lower) probability of positive response to intervention.

AJRCCM Articles in Press. Published on 08-February-2018 as 10.1164/rccm.201708-1728OC

ABSTRACT

Background: It remains unclear how prone positioning improves survival in acute respiratory distress syndrome (ARDS). Using serial computed tomography (CT), we previously reported that 'unstable' inflation, *i.e*. partial aeration with large tidal density swings (indicating increased local strain) is associated with injury progression. We prospectively tested whether prone position contains the early propagation of experimental lung injury by stabilizing inflation.

Methods: Injury was induced by tracheal hydrochloric acid (HCl) in rats; after randomization to supine or prone position, injurious ventilation was commenced using high tidal volume and low PEEP. Paired end-inspiratory (EI) and end-expiratory (EE) CT scans were acquired at baseline and hourly up to 3 hours. Each sequential pair (EI, EE) of CT images was superimposed in parametric response maps to analyze inflation. Unstable inflation was then measured in each voxel in both dependent and non-dependent lung. In addition, 5 pigs were imaged (EI and EE) prone *vs*. supine, before and (one hour) after HCl aspiration.

Results: In rats, prone position limited lung injury propagation and increased survival (11/12 *vs*. 7/12 supine, P=0.01). EI-EE densities, respiratory mechanics, and blood gases deteriorated more in supine vs. prone rats. At baseline, more voxels with unstable inflation occurred in dependent *vs*. non-dependent regions when supine (41$\pm$6% *vs*. 18$\pm$7%, P<0.01), but not when prone. In supine pigs, unstable inflation predominated in dorsal regions and was attenuated by prone positioning.

Conclusions: Prone position limits the radiological progression of early lung injury. Minimizing unstable inflation in this setting may alleviate the burden of ARDS.

INTRODUCTION

Secondary lung injury caused by mechanical ventilation increases mortality in acute respiratory distress syndrome (ARDS) (1–3). Because clinical trials of ventilator strategy in ARDS over the last 15 years have not substantially improved on mortality, new strategies for reducing ventilator-associated lung injury (VALI) are needed.

While ventilating patients in the prone position increases survival (4), the improved gas exchange associated with this strategy (5) does not explain the survival benefit (6). Imaging studies using quantitative computed tomography (CT) (7) and positron emission tomography (8) report that prone positioning attenuates vertical gradients of aeration observed while supine. Such recruitment of atelectatic lung might lessen secondary VALI by reducing regional strain during inspiration (9). However, it is not known if the homogeneity of inflation in the prone position is responsible for attenuating the progression of lung injury; this is potentially important for clinical management, as attenuation in the early stages might lessen the burden of established ARDS.

In our previous studies of experimental ARDS, we used sequential CT imaging to show that regional lung strain drives the propagation of early lung injury (10). Tidal inflation was imaged after primary injury, and the resultant parametric response maps of paired CT scans (*i.e*. paired scans at end-inspiration and at end-expiration) showed areas with partially aerated voxels and large tidal swings in tissue density. We termed this ‘unstable inflation’, and it was associated with the radiological propagation of secondary lung injury. Moreover, in both experimental lung injury and in patients with ARDS, the proportion of (voxels with) unstable inflation was directly related to the extent of injury progression (10).

AJRCCM Articles in Press. Published on 08-February-2018 as 10.1164/rccm.201708-1728OC

In the current study, we used these insights to explore the mechanisms of protection afforded by prone (*vs*. supine) positioning in early lung injury. By linking the regional distribution of inflation with the subsequent trajectory of injury, we were able to successfully test two hypotheses. *First*, ventilation in the prone position limits the early progression of secondary lung injury following a primary insult; *second*, this effect is related to a reduction of the vertical gradients of unstable inflation associated with supine positioning. In an additional series of ventilated pigs, we verified the effects of prone position on unstable inflation in a large animal model. Some of these results have been presented in abstract form (11, 12).

METHODS

Outline: All animal studies were approved by the Animal Care and Use Committee of the University of Pennsylvania. The outline of the small animal experiments is illustrated in ***Figure 1.*** Methodological details are fully described in the Online Data Supplement.

Animal Preparation - Rats: 24 Male Sprague-Dawley rats (365$\pm$21 g) were anesthetized with intraperitoneal pentobarbital, orally intubated, and paralyzed with pancuronium bromide. The carotid artery was catheterized. Heart rate and oxygen saturation (SpO_2) were monitored by pulse-oximetry.

Mechanical Ventilation: Animals were ventilated with tidal volume (V_T; 6 $mL \cdot kg^{-1}$) and positive end-expiratory pressure (PEEP; 10 cmH_2O) using a custom built ventilator(13). Peak inspiratory airway pressure (PIP) and PEEP were recorded, and dynamic compliance was calculated as $C_{dyn} = V_T \cdot (PIP\text{-}PEEP)^{-1}$.

Lung Injury: All rats received 2.5 $mL \cdot kg^{-1}$ hydrochloric acid (HCl, pH 1.25) through the endotracheal tube in two aliquots (10, 14), while in the right and left lateral decubitus. After one hour of supine stabilization (V_T 6 $mL \cdot kg^{-1}$, PEEP 10 cmH_2O), rats were randomized to ventilation in supine or prone position (12 rats in each group) for up to 3 hours, using settings known to induce secondary VALI (10, 14): V_T 12 $mL \cdot kg^{-1}$, PEEP 3 cmH_2O, FiO_2 1.0, and frequency 53 min^{-1}.

Small Animal Imaging: Whole lung computed tomography (CT) was performed at baseline (when stabilized after HCl) and hourly thereafter. Imaging was performed at end inspiration (EI) and end-expiration (EE). In the prone group, additional supine images were obtained at baseline to allow between-group comparisons of primary injury severity.

Image Analysis: The lung boundaries were semi-automatically delineated using a previously developed algorithm (15), yielding whole-lung 'Regions of Interest'. EI and EE images were registered (aligned) to each other using methodology to superimpose anatomical features when distorted by respiration (10). To assess the effect of gravity and position on regional inflation (and on lung injury progression), lungs were partitioned into three coronal bins of equal thickness (ventral, middle and dorsal). Parametric response maps were then generated for the whole lung, as well as for each bin by matching individual voxels in each set of paired EI and EE images (10, 16–19). Voxels were categorized as *severe injury* if both EI and EE densities were >-300 HU, indicating pulmonary edema and stable atelectasis, and as *unstable inflation* if densities fell in the range (EE: 0 to -600 HU, EI: −300 to −700 HU) that we previously found to indicate a high probability of injury progression (10).

AJRCCM Articles in Press. Published on 08-February-2018 as 10.1164/rccm.201708-1728OC

Large Animals: Five Yorkshire pigs (32.4±2.7 kg) were anesthetized, intubated, ventilated with V_T 8 mL·kg^{-1}, and received tracheal HCl (pH 1.25, mL·kg^{-1} into each lung). EI and EE CT scans were obtained at baseline and one hour after HCl, during ventilation in prone and supine position and with PEEP 5 and 10 cmH_2O. All images were analyzed as described for the rats.

Statistical Analysis: Image analysis was performed using Matlab 2016b software applications developed in the authors' laboratory. Statistical analysis was performed using 'R' (R Foundation for Statistical Computing, Vienna, Austria). Group mean and standard deviation of all the computed quantities were calculated. *Post hoc t*-tests were used to identify differences among means, and Bonferroni adjustment was performed. The Fisher exact test was used for proportions. P<0.05 was considered statistically significant.

RESULTS

SMALL ANIMAL STUDIES

Survival: Ventilation in the prone position significantly improved survival; five rats in the supine group died between 2 and 3 hours of ventilation, compared to one in the prone group (Fisher, P=0.013).

Respiratory and Vital Parameters: Compliance (***Figure 2-A***) and driving pressure (***Table 1***) were comparable between groups at baseline. In the supine group, compliance decreased at one hour and again at two hours of ventilation (P<0.01 vs. baseline), reaching lower values than in the prone group (P<0.01 at both times) (***Figure 2-A***).

Baseline oxygenation was similar between groups (***Table 1***), but PaO_2 was lower in the supine than in the prone group after one hour of ventilation (P<0.01), and further decreased in the supine group over time. No significant effect of time or body position on $PaCO_2$ was detected. Oxygen saturation followed a similar trend to PaO_2 (***Table 1***). Blood pH was lower in the supine group than in the prone group after one hour of ventilation (P<0.05) due to higher lactic acid concentration in the former group (***Table 1***).

Arterial blood pressure decreased from baseline after two hours of ventilation in both groups (P<0.01), although it was higher in prone than in supine rats at this time (***Table 1***).

Distribution & Progression of Lung Injury: Baseline CT scans, obtained supine in both groups, confirmed that the distribution of primary injury was similar and that primary lesions were dorsal, irrespective of group assignment (***Figure 3***).

In supine animals, injury propagated rapidly over the entire lung (***Figure 3***-Upper), as previously described (10). Changing from supine to prone position resulted in the attenuation of dorsal hyperdensities, which remained stable thereafter for the duration of the experiment (***Figure 3***-Lower).

Quantitative CT analysis demonstrated that both EI and EE lung gas volumes were smaller in supine *vs*. prone animals during the course of the experiment (P<0.01); both EI and EE values also decreased to a greater extent in supine vs. prone rats (***Figure 2-B***). CT estimates of lung weight (reflecting tissue edema) increased only in the supine group (***Figure 2-C***).

Baseline parametric response maps in the supine position were similar in the two groups, indicating comparable inflation conditions after the primary (acid instillation) lung injury (***Figure 4***). At each subsequent time point, maps showed an evolving distribution of voxels in the supine

AJRCCM Articles in Press. Published on 08-February-2018 as 10.1164/rccm.201708-1728OC

group (***Figure 4****-top panels*), with more voxels developing in the higher (>-300 HU) domains of EI and EE density, indicating *severe injury* (square); voxels with reversible expiratory loss of gas content (indicating cyclic recruitment) appeared only after one hour of ventilation (arrow). Low-density voxels were prevalent at all times in the prone rats, and density distribution evolved only minimally (***Figure 4***-bottom panels). Categorization of voxels showed a progressive increase in the fraction of *unstable inflation* voxels in supine (baseline: 28.5±6.7%; end: 44.1±22.8%, P<0.01), but not in prone position (baseline: 26.9±3.2%; end: 28.7±4.9%, P=0.35). Representative EI-EE images are shown in Figure E1.

Regional Injury: Analysis of the three horizontal bins showed that time-dependent increases of EI-EE density were more prominent in the dependent (*i.e*. dorsal) *vs*. non-dependent lung in the supine group (***Figure 5***).

In baseline supine scans, the averaged voxel distribution was of lower density in non-dependent lung regions, and of higher density in the dependent lung (***Figure 5***). This 'shift' was characterized by the changing position of the 'distribution centroid' (***Figure 5-dashed line***).

In the prone position, minimal gravity-related change of the voxel distributions (or the respective centroids) was observed (***Figure 5***), and evolution was comparable between dependent (ventral) and non-dependent (dorsal) bins.

Categorization of voxel distribution at baseline showed that 'unstable inflation' and 'severely injured' voxels were significantly affected by gravity in the supine position, but not in the prone position (***Figure 6-A***). In supine animals, significantly higher fractions of 'unstable inflation' and *severe injury* tissue voxels were present in the dependent (dorsal) regions of the lungs compared to the other regions.

Finally, the baseline fraction of '*unstable inflation'* voxels in the dorsal bins (dependent in supine, non-dependent in prone) was positively correlated with the decrease in respiratory system compliance (R=0.71; ***Figure 6-B***), but not with *'severe injury'*.

LARGE ANIMAL STUDIES

In the pig experiments, HCl aspiration caused mild oxygenation impairment, worsened mechanics, and relatively small dorsal hyperdensities on CT (***Table E1, Figure E2,*** Online Data Supplement). Prone positioning attenuated both functional abnormalities and dorsal opacities. After HCl, parametric response maps showed the appearance of more voxels with unstable inflation in the dorsal bin (***Figure 7, Figure E4***). This abnormal inflation was attenuated but not abolished in the prone position with PEEP 5 cmH_2O. PEEP 10 cmH_2O also produced a decrease in dorsal voxels with unstable inflation, but inflation distribution was further improved in the prone position.

DISCUSSION

In this study, prone positioning limited the early propagation of radiological abnormalities after experimental lung injury and improved survival during mechanical ventilation. The effect of prone positioning was likely related to its ability to decrease areas of unstable inflation in the dependent regions of the lungs. Thus, prone positioning could prevent severe ARDS by protecting the lungs from the progression of injury in its early stages.

While prone positioning has been introduced as a rescue therapy for severely hypoxemic ARDS (20–22), the improved oxygenation which it produces does not explain the observed improvement in survival among patients with severe ARDS (6). Using serial CT, our study

AJRCCM Articles in Press. Published on 08-February-2018 as 10.1164/rccm.201708-1728OC

showed that prone positioning reduced the regional propagation of CT densities compared to supine positioning, while also attenuating the deterioration of respiratory mechanics and development of pulmonary edema (estimated from tissue weight). These results suggest that prone positioning may improve ARDS outcomes by alleviating the early evolution of 'secondary' (ventilator-associated) lung injury, before it becomes severe.

In a previous study of mechanical ventilation with non-protective settings in experimental ARDS (14), we reported that radiological propagation is the visual manifestation of evolving lung injury. Using analysis of longitudinal CT scans in a similar model (10), we then observed that this secondary propagation was more severe in lungs that displayed larger areas of tissue with unstable inflation. In that same study, unstable inflation was also found to be associated with higher mortality in a small group of patients with early ARDS (10). Partial inflation includes areas with stable poor aeration, but it is dominated by large tidal density changes within partially aerated tissue. Studies using diffusion MRI suggest that this pattern of inflation indicates overstretched airspaces embedded in voxels with reduced (but not abolished) gas content (13, 23, 24). While unstable inflation may be simply a marker of heterogeneous gas distribution, such stress concentration can regionally increases the risk of VALI (25, 26). Unstable inflation is distinct from cyclic recruitment of atelectasis, which is defined as complete but reversible loss of aeration (27). As with unstable inflation, cyclic recruitment was not correlated with propagation of injury after acid aspiration (14).

In the current study, regional analysis revealed a vertical gradient of abnormal inflation in supine rats that was not present in prone rats. Voxels with unstable inflation were more abundant in the dependent (dorsal) lung of supine rats, where the radiological signs of both

primary injury and its progression were more visible. We also observed that, irrespective of body position, the baseline fraction of unstable inflation in the dorsal lung predicted worsening mechanics (***Figure 6-B***). Overall, the findings of this study suggest that prone positioning reduced the harmful effects of mechanical ventilation in dependent regions of tissue with unstable inflation, thereby mitigating the radiological propagation of the injury to the rest of the lung. Further studies will be needed to confirm that tissue inflammation is attenuated by this strategy.

Other authors have studied the effects of the prone position on regional lung mechanics and VALI, finding that prone position attenuated vertical gradients of pleural pressure and regional strain, in addition to improving dorsal atelectasis (28, 29) and ventral hyperinflation (30). Using CT in established ARDS, prone position was shown to augment recruitment by PEEP (9). Nuclear medicine studies have shown less heterogeneity of both lung aeration and perfusion in prone vs. supine sheep with surfactant depletion (31). Another study showed that prone position delayed the progression of lung injury in previously healthy lungs receiving high stretch ventilation (32), supporting a causal relation between improved mechanics and milder injury. Finally, in a study of pre-injured lungs (oleic acid) receiving ventilation with elevated inflation pressure, prone positioning attenuated injury in the dorsal lung (33), suggesting that attenuation of airspace collapse in dependent regions may be crucial to the success of positional therapy.

Our work differs from these previous studies (9, 28–32, 34) in that it is the first to demonstrate that prone positioning can attenuate the radiological and functional progression of lung injury, before it becomes established and severe. This finding was enabled by our use of

AJRCCM Articles in Press. Published on 08-February-2018 as 10.1164/rccm.201708-1728OC

longitudinal imaging, which allowed us to link unstable inflation, future propagation of lung injury, and response to body position. Furthermore, our model recapitulates the early evolution of lung injury, when hypoxemia is still mild and radiological abnormalities are spatially limited. Our short-term studies in pigs showed that, similar to the rats, prone position decreased unstable inflation in the dorsal lung, supporting long term experiments to test this approach in large animals. Similar to our previous studies (10, 14), we used a model of secondary VALI superimposed on mild primary injury, as indicated by the relatively mild oxygenation impairment at one hour after acid aspiration in both rat cohorts (***Table 1***). In addition to helping understand how positional therapy improves outcomes, this study's findings suggest a potential new use for prone positioning: it could be used in patients with early lung injury to prevent the development of severe ARDS.

In a clinical trial which recruited only patients with severe hypoxemia, Guerin et al. reported better outcomes with prone *vs*. supine position (4); in contrast, outcomes were mixed in earlier clinical trials that included patients with less severe ARDS (35). However, this does not mean that prone position is ineffective in carefully selected subjects with milder hypoxemia, as the discrepancy may be related to heterogeneity of patient characteristics within the study populations (36). In fact, a one-time measurement of oxygenation impairment is a worse prognostic indicator than either treatment responsiveness (37) or imaging-derived metrics (10, 38). While we do not yet propose clinical implementation of this evidence, the current study suggests that the effectiveness of prone position may be related to the characteristics described in the dependent lung. In addition to CT scanning, other methodologies (*e.g*. lung

ultrasound (39), and electrical impedance tomography (40)) may allow for the efficient measurement of unstable dorsal inflation in order to assess the early risk of injury progression.

There are several limitations inherent to this study. *First*, as shown by our previous studies, injury progression is variable in this animal model, and could be affected by inter-group differences of baseline severity rather than by treatment. However, measured treatment effects were large, and the primary injury was consistent between groups. In addition, the baseline images obtained while supine showed similar injury morphology in animals before randomization into prone and supine cohorts (***Figure 3***) and in parametric response maps (***Figures 4*** *and* ***5***).

Second, we used non-protective ventilator settings (i.e. large tidal volume and low PEEP). The choice of such settings diminishes the clinical relevance of our study, but was motivated by the need to visualize injury progression within the time frame of the experiment. However, relatively high tidal volumes and low PEEP continue to be used in clinical practice (1). Smaller tidal volumes and higher PEEP could have attenuated injury, while redistributing mixed and heterogeneous aeration to more ventral lung regions (41) as a consequence of dorsal recruitment. However, in the pig studies (V_T 8 mL·kg^{-1}), dorsal unstable inflation persisted at PEEP 10 cmH_2O and was decreased by prone positioning; the efficacy of prone positioning thus was maintained at higher PEEP levels (***Figure 7, Figure E4*** in the Online Data Supplement).

Third, the dorsal lung was more involved by the primary injury, which was an intentional consequence of the HCl injection technique meant to mimic human aspiration injury. The efficacy of position with other injury distributions (*e.g*. ventral predominance) was not explored

AJRCCM Articles in Press. Published on 08-February-2018 as 10.1164/rccm.201708-1728OC

in the current study, and could be different if prone position does not improve regional inflation patterns.

Finally, the rat model may be less affected by gravity than larger animals and humans. Inflation distribution may be governed by changes in thoracic geometry rather than by gravity vector (32), as suggested by the larger chest wall diameters in prone *vs*. supine rats (***Table E2***, Online Data Supplement). Irrespective of the mechanism, however, we were able to find vertical gradients of inflation distribution in rats which qualitatively resembled those observed in the pigs. We may expect similar effects of prone positioning on injury propagation in large animal models, although this needs verification.

We used radiological and functional variables as surrogates for tissue inflammation, rather than attempting direct measurements. The distributions of histological injury and radiological densities are similar in spatially matched tissue and CT slices (14). Furthermore, respiratory compliance is a surrogate of VALI in animal models (42). Further studies are required to characterize the spatial relationships between *'severe injury'*, *'unstable inflation'* and tissue inflammation. While lung inflammation is often detectable in the non-dependent, lung that receive most of inspired gas (43–45), this may be a characteristic of established ARDS: studies on the early stages of injury showed inflammation in dependent lung regions with poor aeration, which could be a consequence of local stress (46). Mechanisms other than redistribution of inflation and attenuation of VALI may influence the effects of prone positioning on injury progression. These include reduced secretions and increased bacterial clearance , as well as reduced blood flow to areas of injury (47). Furthermore, reduced cardiac output could decrease capillary perfusion and lessen pulmonary edema. However, mean

intrathoracic pressure was likely similar in both positions, as the same ventilator settings were maintained in both conditions. In addition, blood pressure was greater (and lactate lower) in the prone position, suggesting hemodynamic advantage as previously described (48). Finally, left heart failure, hypotension, and acute *cor pulmonale* could have exacerbated edema and caused greater mechanical impairment in the supine group (49).

CONCLUSION

This experimental study indicates that prone position attenuates the trajectory of early lung injury, suggesting a possible use of this strategy in selected patients, to prevent progression to severe ARDS. Further experimental and clinical studies are required to confirm whether unstable inflation can be used as a predictor of both ARDS progression and of treatment success.

AJRCCM Articles in Press. Published on 08-February-2018 as 10.1164/rccm.201708-1728OC

REFERENCES

1. Bellani G, Laffey JG, Pham T, Fan E, Brochard L, Esteban A, Gattinoni L, van Haren F, Larsson A, McAuley DF, Ranieri M, Rubenfeld G, Thompson BT, Wrigge H, Slutsky AS, Pesenti A, Investigators LS, Group ET. Epidemiology, Patterns of Care, and Mortality for Patients With Acute Respiratory Distress Syndrome in Intensive Care Units in 50 Countries. JAMA 2016;315:788–800.
2. Network TARDS. Ventilation with Lower Tidal Volumes as Compared with Traditional Tidal Volumes for Acute Lung Injury and the Acute Respiratory Distress Syndrome. N Engl J Med 2000;342:1301–1308.
3. Slutsky AS, Ranieri VM. Ventilator-Induced Lung Injury. N Engl J Med 2013;369:2126–2136.
4. Guérin C, Reignier J, Richard J-C, Beuret P, Gacouin A, Boulain T, Mercier E, Badet M, Mercat A, Baudin O, Clavel M, Chatellier D, Jaber S, Rosselli S, Mancebo J, Sirodot M, Hilbert G, Bengler C, Richecoeur J, Gainnier M, Bayle F, Bourdin G, Leray V, Girard R, Baboi L, Ayzac L. Prone Positioning in Severe Acute Respiratory Distress Syndrome. N Engl J Med 2013;368:2159–2168.
5. Gattinoni L, Tognoni G, Pesenti A, Taccone P, Mascheroni D, Labarta V, Malacrida R, Di Giulio P, Fumagalli R, Pelosi P, others. Effect of prone positioning on the survival of patients with acute respiratory failure. N Engl J Med 2001;345:568–573.
6. Albert RK, Keniston A, Baboi L, Ayzac L, Guérin C. Prone position–induced improvement in gas exchange does not predict improved survival in the acute respiratory distress syndrome. Am J Respir Crit Care Med 2014;189:494–496.
7. Pelosi P, Brazzi L, Gattinoni L. Prone position in acute respiratory distress syndrome. Eur Respir J 2002;20:1017–1028.
8. Musch G, Layfield JDH, Harris RS, Melo MFV, Winkler T, Callahan RJ, Fischman AJ, Venegas JG. Topographical distribution of pulmonary perfusion and ventilation, assessed by PET in supine and prone humans. J Appl Physiol 2002;93:1841–1851.
9. Cornejo RA, Díaz JC, Tobar EA, Bruhn AR, Ramos CA, González RA, Repetto CA, Romero CM, Gálvez LR, Llanos O, Arellano DH, Neira WR, Díaz GA, Zamorano AJ, Pereira GL. Effects of Prone Positioning on Lung Protection in Patients with Acute Respiratory Distress Syndrome. Am J Respir Crit Care Med 2013;188:440–448.
10. Cereda M, Xin Y, Hamedani H, Bellani G, Kadlecek S, Clapp J, Guerra L, Meeder N, Rajaei J, Tustison NJ, Gee JC, Kavanagh BP, Rizi RR. Tidal changes on CT and progression of ARDS. Thorax 2017; 72:981-989.
11. Xin Y, Cereda M, Hamedani H, Siddiqui S, Pourfathi M, Itkin-Ofer M, Turner S, Meeder N, Kadlecek S, Clapp J, Hughes L, Roberts A, Bey Q, Rodriguez A, Drachman N, Duncan I, Profka H, Tustison N, Gee J, Kavanagh BP, Rizi RR. Parametric Response Maps to Measure the Effects of Prone Position in Pigs with Experimental Lung Injury [abstract]. Am J Respir Crit Care Med 2017;195: A3749
12. Cereda M, Xin Y, Meeder N, Zeng J, Rodriguez A, Staroba H, Bey Q, Profka H, Kadlecek S, Kavanagh BP, Wu J, Gee JC, Rizi RR: Parametric Response Mapping for the Analysis of Regional Inflation in the Prone Position [abstract]. Am J Respir Crit Care Med 2016; 193:A4411

13. Cereda M, Emami K, Xin Y, Kadlecek S, Kuzma NN, Mongkolwisetwara P, Profka H, Pickup S, Ishii M, Kavanagh BP, Deutschman CS, Rizi RR. Imaging the Interaction of Atelectasis and Overdistension in Surfactant-Depleted Lungs: Crit Care Med 2013;41:527–535.
14. Cereda M, Xin Y, Meeder N, Zeng J, Jiang Y, Hamedani H, Profka H, Kadlecek S, Clapp J, Deshpande CG, others. Visualizing the Propagation of Acute Lung Injury. Anesthesiology 2016;124:121–131.
15. Xin Y, Song G, Cereda M, Kadlecek S, Hamedani H, Jiang Y, Rajaei J, Clapp J, Profka H, Meeder N, Wu J, Tustison NJ, Gee JC, Rizi RR. Semiautomatic segmentation of longitudinal computed tomography images in a rat model of lung injury by surfactant depletion. J Appl Physiol 2015;118:377–385.
16. Galbán CJ, Han MK, Boes JL, Chughtai KA, Meyer CR, Johnson TD, Galbán S, Rehemtulla A, Kazerooni EA, Martinez FJ, Ross BD. Computed tomography–based biomarker provides unique signature for diagnosis of COPD phenotypes and disease progression. Nat Med 2012;18:1711–1715.
17. Avants B, Epstein C, Grossman M, Gee J. Symmetric diffeomorphic image registration with cross-correlation: Evaluating automated labeling of elderly and neurodegenerative brain. Med Image Anal 2008;12:26–41.
18. Song G, Tustison N, Avants B, Gee JC. Lung CT image registration using diffeomorphic transformation models. Med Image Anal Clin Gd Chall 2010;23–32.
19. Tustison NJ, Avants BB. Explicit B-spline regularization in diffeomorphic image registration. Front Neuroinformatics 2013;7:.
20. Bryan AC. Comments of a devil's advocate. Am Rev Respir Dis 1974;110:143–144.
21. Blanch L, Mancebo J, Perez M, Martinez M, Mas A, Betbese AJ, Joseph D, Ballús J, Lucangelo U, Bak E. Short-term effects of prone position in critically ill patients with acute respiratory distress syndrome. Intensive Care Med 1997;23:1033–1039.
22. Langer M, Mascheroni D, Marcolin R, Gattinoni L. The Prone Position in ARDS Patients. Chest 1988;94:103–107.
23. Cereda M, Emami K, Kadlecek S, Xin Y, Mongkolwisetwara P, Profka H, Barulic A, Pickup S, Mansson S, Wollmer P, Ishii M, Deutschman CS, Rizi RR. Quantitative imaging of alveolar recruitment with hyperpolarized gas MRI during mechanical ventilation. J Appl Physiol 2011;110:499–511.
24. Cereda M, Xin Y, Hamedani H, Clapp J, Kadlecek S, Meeder N, Zeng J, Profka H, Kavanagh BP, Rizi RR. Mild loss of lung aeration augments stretch in healthy lung regions. J Appl Physiol 2016;120:444–454.
25. Mead J, Takishima T, Leith D. Stress distribution in lungs: a model of pulmonary elasticity. J Appl Physiol 1970;28:596–608.
26. Retamal J, Bergamini BC, Carvalho AR, Bozza FA, Borzone G, Borges JB, Larsson A, Hedenstierna G, Bugedo G, Bruhn A. Non-lobar atelectasis generates inflammation and structural alveolar injury in the surrounding healthy tissue during mechanical ventilation. Crit Care 2014;18:505.
27. Chiumello D, Marino A, Brioni M, Cigada I, Menga F, Colombo A, Crimella F, Algieri I, Cressoni M, Carlesso E, Gattinoni L. Lung Recruitment Assessed by Respiratory Mechanics and Computed Tomography in Patients with Acute Respiratory Distress Syndrome. What Is the Relationship? Am J Respir Crit Care Med 2016;193:1254–1263.

AJRCCM Articles in Press. Published on 08-February-2018 as 10.1164/rccm.201708-1728OC

28. Gattinoni L, Pelosi P, Vitale G, Pesenti A, D'Andrea L, Mascheroni D. Body position changes redistribute lung computed-tomographic density in patients with acute respiratory failure. Anesthesiology 1991;74:15–23.
29. MUTOH T, Guest J, Lamm JE, Albert RK. Prone Position Alters the Effect of Volume Overload on Regional Pleural Pressures and Improves Hypoxemia in Pigs In ViV01, 2. Am Rev Respir Dis 1992;146:300–306.
30. Galiatsou E, Kostanti E, Svarna E, Kitsakos A, Koulouras V, Efremidis SC, Nakos G. Prone Position Augments Recruitment and Prevents Alveolar Overinflation in Acute Lung Injury. Am J Respir Crit Care Med 2006;174:187–197.
31. Richter T, Bellani G, Harris RS, Melo MFV, Winkler T, Venegas JG, Musch G. Effect of Prone Position on Regional Shunt, Aeration, and Perfusion in Experimental Acute Lung Injury. Am J Respir Crit Care Med 2005;172:480–487.
32. Valenza F, Guglielmi M, Maffioletti M, Tedesco C, Maccagni P, Fossali T, Aletti G, Porro GA, Irace M, Carlesso E, Carboni N, Lazzerini M, Gattinoni L. Prone position delays the progression of ventilator-induced lung injury in rats: Does lung strain distribution play a role?*: Crit Care Med 2005;33:361–367.
33. Broccard AF, Shapiro RS, Schmitz LL, Ravenscraft SA, Marini JJ. Influence of prone position on the extent and distribution of lung injury in a high tidal volume oleic acid model of acute respiratory distress syndrome. Crit Care Med 25:16–27.
34. Perchiazzi G, Rylander C, Vena A, Derosa S, Polieri D, Fiore T, Giuliani R, Hedenstierna G. Lung regional stress and strain as a function of posture and ventilatory mode. J Appl Physiol 2011;110:1374–1383.
35. Sud S, Friedrich JO, Taccone P, Polli F, Adhikari NKJ, Latini R, Pesenti A, Guérin C, Mancebo J, Curley MAQ, Fernandez R, Chan M-C, Beuret P, Voggenreiter G, Sud M, Tognoni G, Gattinoni L. Prone ventilation reduces mortality in patients with acute respiratory failure and severe hypoxemia: systematic review and meta-analysis. Intensive Care Med 2010;36:585–599.
36. Rubenfeld GD. Confronting the Frustrations of Negative Clinical Trials in Acute Respiratory Distress Syndrome. Ann Am Thorac Soc 2015;12:S58–S63.
37. Goligher EC, Kavanagh BP, Rubenfeld GD, Adhikari NKJ, Pinto R, Fan E, Brochard LJ, Granton JT, Mercat A, Marie Richard J-C, Chretien J-M, Jones GL, Cook DJ, Stewart TE, Slutsky AS, Meade MO, Ferguson ND. Oxygenation response to positive end-expiratory pressure predicts mortality in acute respiratory distress syndrome. A secondary analysis of the LOVS and ExPress trials. Am J Respir Crit Care Med 2014;190:70–76.
38. Gattinoni L, Caironi P, Cressoni M, Chiumello D, Ranieri VM, Quintel M, Russo S, Patroniti N, Cornejo R, Bugedo G. Lung Recruitment in Patients with the Acute Respiratory Distress Syndrome. N Engl J Med 2006;354:1775–1786.
39. Wang X-T, Ding X, Zhang H-M, Chen H, Su L-X, Liu D-W, Chinese Critical Ultrasound Study Group (CCUSG). Lung ultrasound can be used to predict the potential of prone positioning and assess prognosis in patients with acute respiratory distress syndrome. Crit Care Lond Engl 2016;20:385.
40. Mauri T, Eronia N, Turrini C, Battistini M, Grasselli G, Rona R, Volta CA, Bellani G, Pesenti A. Bedside assessment of the effects of positive end-expiratory pressure on lung inflation and recruitment by the helium dilution technique and electrical impedance tomography. Intensive Care Med 2016;42:1576–1587.

41. Cressoni M, Cadringher P, Chiurazzi C, Amini M, Gallazzi E, Marino A, Brioni M, Carlesso E, Chiumello D, Quintel M, Bugedo G, Gattinoni L. Lung inhomogeneity in patients with acute respiratory distress syndrome. Am J Respir Crit Care Med 2014;189:149–158.
42. Sibilla S, Tredici S, Porro G, Irace M, Guglielmi M, Nicolini G, Tredici G, Valenza F, Gattinoni L. Equal increases in respiratory system elastance reflect similar lung damage in experimental ventilator-induced lung injury. Intensive Care Med 2002;28:196–203.
43. Bellani G, Guerra L, Musch G, Zanella A, Patroniti N, Mauri T, Messa C, Pesenti A. Lung Regional Metabolic Activity and Gas Volume Changes Induced by Tidal Ventilation in Patients with Acute Lung Injury. Am J Respir Crit Care Med 2011;183:1193–1199.
44. Borges JB, Costa ELV, Suarez-Sipmann F, Widström C, Larsson A, Amato M, Hedenstierna G. Early inflammation mainly affects normally and poorly aerated lung in experimental ventilator-induced lung injury*. Crit Care Med 2014;42:e279-287.
45. Tsuchida S, Engelberts D, Peltekova V, Hopkins N, Frndova H, Babyn P, McKerlie C, Post M, McLoughlin P, Kavanagh BP. Atelectasis causes alveolar injury in nonatelectatic lung regions. Am J Respir Crit Care Med 2006;174:279–289.
46. Wellman TJ, Prost N de, Tucci M, Winkler T, Baron RM, Filipczak P, Raby B, Chu J, Harris RS, Musch G, Falcao LF dos R, Capelozzi V, Venegas JG, Melo MFV. Lung Metabolic Activation as an Early Biomarker of Acute Respiratory Distress Syndrome and Local Gene Expression Heterogeneity. Anesthesiol J Am Soc Anesthesiol 2016;125:992–1004.
47. Broccard AF, Hotchkiss JR, Kuwayama N, Olson DA, Jamal S, Wangensteen DO, Marini JJ. Consequences of vascular flow on lung injury induced by mechanical ventilation. Am J Respir Crit Care Med 1998;157:1935–1942.
48. Vieillard-Baron A, Charron C, Caille V, Belliard G, Page B, Jardin F. Prone positioning unloads the right ventricle in severe ARDS. Chest 2007;132:1440–1446.
49. Katira BH, Giesinger RE, Engelberts D, Zabini D, Kornecki A, Otulakowski G, Yoshida T, Kuebler WM, McNamara PJ, Connelly KA, Kavanagh BP. Adverse Heart-lung Interactions in Ventilator-induced Lung Injury. Am J Respir Crit Care Med 2017;doi:10.1164/rccm.201611-2268OC.

AJRCCM Articles in Press. Published on 08-February-2018 as 10.1164/rccm.201708-1728OC

FIGURE LEGENDS

Figure 1. Experimental timeline in rats ventilated in supine vs. prone position after hydrochloric acid (HCl) aspiration. Identical ventilator settings were used in both groups. In the prone group, additional inspiratory and expiratory CT scans were acquired at baseline (after HCl) in the supine position to assess the acute effects of prone ventilation on inflation distribution and to compare injury distribution with supine ventilation group.

Figure 2. Group statistics (mean and standard deviation) of (A) respiratory system compliance, (B) total lung volumes, and (C) lung mass normalized to baseline. All measurements were obtained at baseline (after HCl) as well as after one and two hours of ventilation. †: $P<0.05$ between cohorts; §: $P<0.05$ vs. baseline in the same group.

Figure 3. Radiological injury propagation in four representative rats ventilated in prone vs. supine position (two rats in each group) and imaged at end-inspiration. Baseline (after HCl) supine images are also shown for the two prone rats (#3 and #4). In all rats, primary injury was initially localized in the dorsal lung regions. In the rats ventilated supine (#1 and #2), injury rapidly spread over the entire lung. In the prone rats, position change improved aeration in the dorsal lung regions (black arrows) and subsequent injury propagation was more contained. The blue triangles indicate body position (up-pointing: supine, down-pointing: prone)

Figure 4. Whole-lung parametric response maps obtained at baseline after HCl aspiration and hourly until the end of the experiment in the two experimental cohorts. Each map shows a cumulative voxel distribution for each condition, obtained by incorporating all rats in each group and averaging the distributions. The blue triangles indicate body position (up-pointing: supine, down-pointing: prone). In the supine rats, maps evolved with increased representation

of voxels with non-reversible high-density (square), indicating edema and/or non-reversible atelectasis (*severe injury*). In this group, voxels with complete expiratory loss of gas content and inspiratory re-aeration (indicating reversible atelectasis) appeared only after one and two hours of ventilation (arrow). In the prone rats, the voxel distributions were more stable over time.

Figure 5. Cumulative parametric response maps of EI-EE voxels partitioned in non-dependent, mid-level, and dependent regions of the lungs (indicated by the solid blue color in the triangle) in the prone and supine position (indicated by the tip of the triangle). In the supine position at baseline, the centroid of the voxel distribution shifted towards higher density following the gravitational gradient. Over time, changes in the voxel distributions were more evident in the dependent lung regions than in the non-dependent ones. In the prone position, the centroid and the voxel distribution changed minimally in the tree regions at baseline (minimal deviation from white vertical reference line); evolution in the dorsal lung regions was less than in the supine rats. The area including voxels with *unstable inflation* is highlighted (green border) in the dorsal maps.

Figure 6. (A) *Unstable inflation* and *severely injured* voxels are shown (as a percent of total) in the non-dependent, mid-level, and dependent lung regions of the baseline images obtained in supine and prone rats. (B) Correlation between change in compliance (between baseline and the end of the experiment) and baseline percent fraction of *unstable inflation* voxels in the dependent lung regions. Solid dots indicate rats that died before two hours of ventilation. †: $P<0.05$ between cohorts.

Figure 7. Cumulative parametric response maps in 5 pigs imaged before and one hour after HCl aspiration. Pigs were ventilated in the prone vs. supine position with tidal volume 8 $mL \cdot kg^{-1}$ and

AJRCCM Articles in Press. Published on 08-February-2018 as 10.1164/rccm.201708-1728OC

PEEP 5 and 10 cmH_2O. Similar to the rats, we observed a gravitational gradient of inflation distribution when the animals were supine, with more representation of unstable inflation voxels in dependent lung after injury. This maldistribution improved at higher PEEP, but it persisted in the supine position. Prone positioning caused a more homogeneous voxel distribution at both PEEP levels.

	Supine			Prone		
	Baseline	**1 hr**	**2 hrs**	**Baseline**	**1 hr**	**2 hrs***
Arterial Blood Pressure (mmHg)	113.8±12.3	108.9±19.9	82.9±41.9 §	126.0±8.4	118.2±23.1	104.8±28.5 §
Driving Pressure (cmH_2O)	19.1±2.9	23.3±5.6 §	28.7±6.6 §	19.9±2.2	20.7±3.3	21.8±4.0 †
pO_2 (mmHg)	396.3±79.7	107.5±56.5 §	43.6±7.5 §	388.8±65.9	217.0±109.3 †§	142.9±108.1
pCO_2 (mmHg)	45.9±8.2	50.0±11.2	50.6±10.2	46.4±6.7	44.8±7.8	48.7±11.1
pH	7.34±0.06	7.26±0.06 §	7.19±0.04 §	7.32±0.07	7.29±0.01	7.30±0.06
SpO_2 (%)	99.9±0.1	94.5±4.9 §	65.9±11.7 §	99.9±0.1	99.0±0.8	94.4±7.5 †§
Blood Lactate ($mmol \cdot L^{-1}$)	1.28±0.40	2.50±1.29 §	4.82±3.26 §	1.54±0.72	1.89±1.38	1.49±0.08

Table 1. Physiological characteristics of two groups of rats ventilated in the prone vs. supine position after hydrochloric acid instillation in the trachea. †: P<0.05 between cohorts; §: P<0.05 vs. baseline in the same group. *: In the prone group, arterial blood gases were available at two hours in only 3 rats due to positional difficulties drawing blood through the carotid catheter after one hour of prone ventilation.

AJRCCM Articles in Press. Published on 08-February-2018 as 10.1164/rccm.201708-1728OC

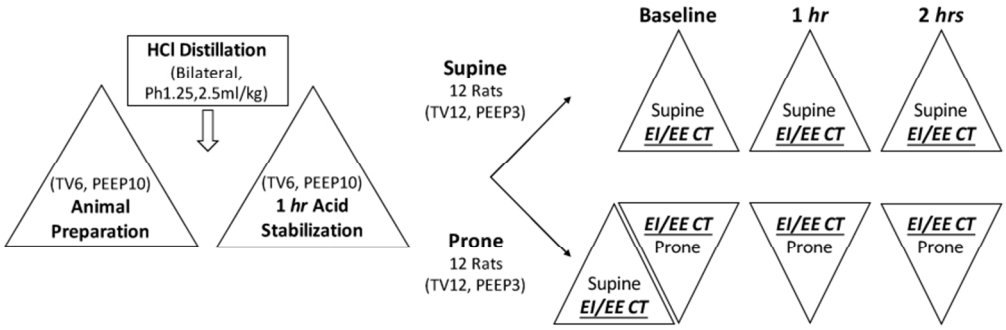

Figure 1. Experimental timeline in rats ventilated in supine vs. prone position after hydrochloric acid (HCl) aspiration. Identical ventilator settings were used in both groups. In the prone group, additional inspiratory and expiratory CT scans were acquired at baseline (after HCl) in the supine position to assess the acute effects of prone ventilation on inflation distribution and to compare injury distribution with supine ventilation group.

316x106mm (72 x 72 DPI)

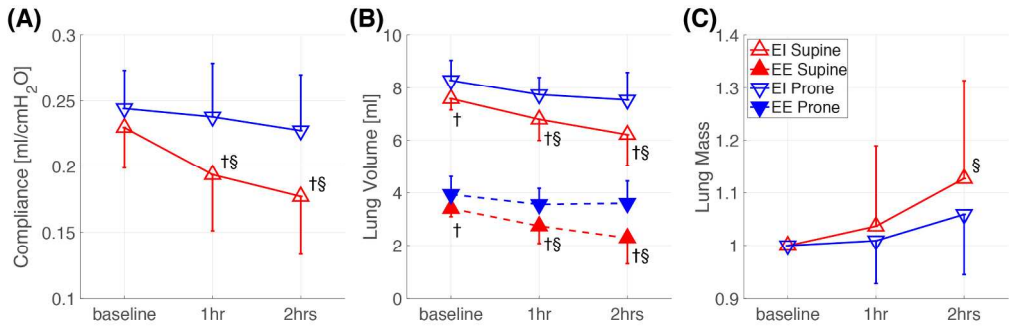

Figure 2. Group statistics (mean and standard deviation) of (A) respiratory system compliance, (B) total lung volumes, and (C) lung mass normalized to baseline. All measurements were obtained at baseline (after HCl) as well as after one and two hours of ventilation. †: P<0.05 between cohorts; §: P<0.05 vs. baseline in the same group.

423x136mm (150 x 150 DPI)

AJRCCM Articles in Press. Published on 08-February-2018 as 10.1164/rccm.201708-1728OC

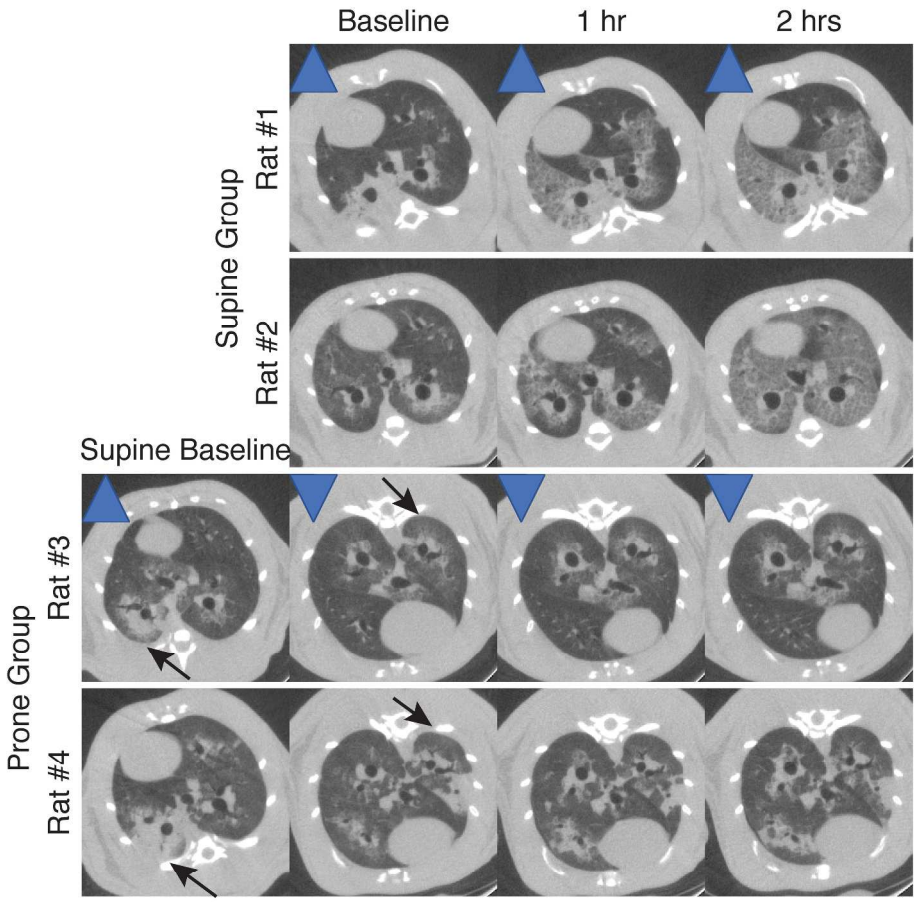

Figure 3. Radiological injury propagation in four representative rats ventilated in prone vs. supine position (two rats in each group) and imaged at end-inspiration. Baseline (after HCl) supine images are also shown for the two prone rats (#3 and #4). In all rats, primary injury was initially localized in the dorsal lung regions. In the rats ventilated supine (#1 and #2), injury rapidly spread over the entire lung. In the prone rats, position change improved aeration in the dorsal lung regions (black arrows) and subsequent injury propagation was more contained. The blue triangles indicate body position (up-pointing: supine, down-pointing: prone).

279x361mm (300 x 300 DPI)

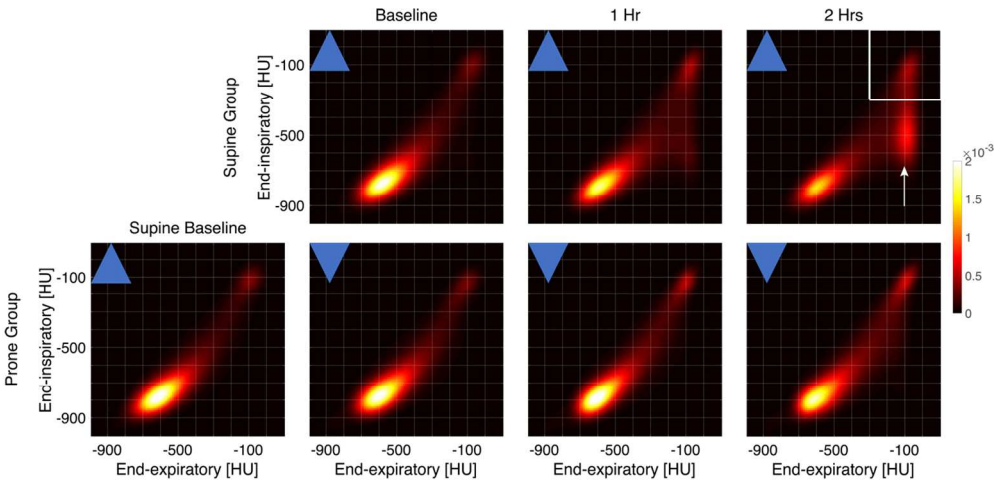

Figure 4. Whole-lung parametric response maps obtained at baseline after HCl aspiration and hourly until the end of the experiment in the two experimental cohorts. Each map shows a cumulative voxel distribution for each condition, obtained by incorporating all rats in each group and averaging the distributions. The blue triangles indicate body position (up-pointing: supine, down-pointing: prone). In the supine rats, maps evolved with increased representation of voxels with non-reversible high-density (square), indicating edema and/or non-reversible atelectasis (severe injury). In this group, voxels with complete expiratory loss of gas content and inspiratory re-aeration (indicating reversible atelectasis) appeared only after one and two hours of ventilation (arrow). In the prone rats, the voxel distributions were more stable over time.

401x191mm (95 x 95 DPI)

AJRCCM Articles in Press. Published on 08-February-2018 as 10.1164/rccm.201708-1728OC

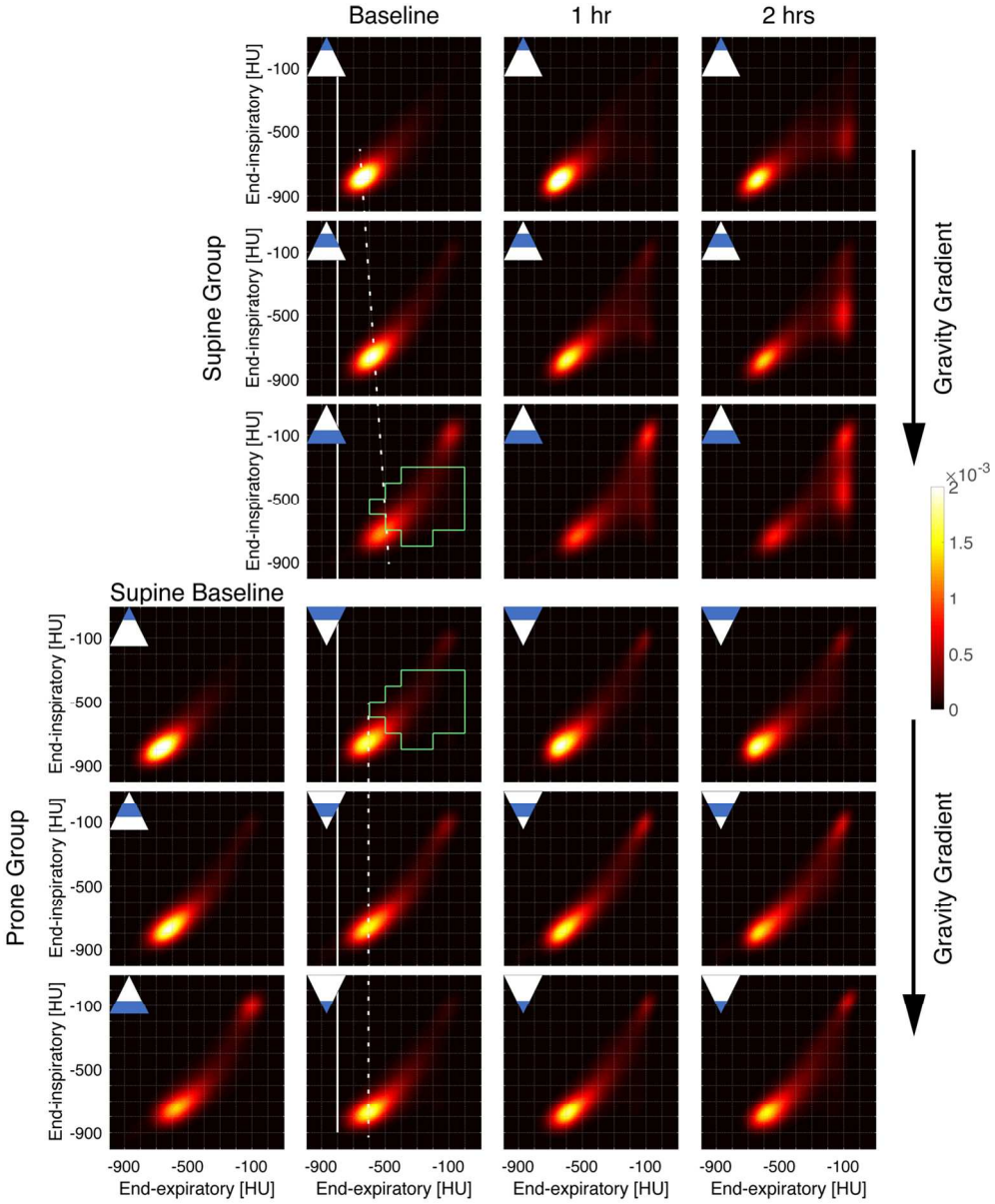

Figure 5. Cumulative parametric response maps of EI-EE voxels partitioned in non-dependent, mid-level, and dependent regions of the lungs (indicated by the solid blue color in the triangle) in the prone and supine position (indicated by the tip of the triangle). In the supine position at baseline, the centroid of the voxel distribution shifted towards higher density following the gravitational gradient. Over time, changes in the voxel distributions were more evident in the dependent lung regions than in the non-dependent ones. In the prone position, the centroid and the voxel distribution changed minimally in the tree regions at baseline (minimal deviation from white vertical reference line); evolution in the dorsal lung regions was less than in the supine rats. The area including voxels with unstable inflation is highlighted (green border) in the dorsal maps.

401x487mm (95 x 95 DPI)

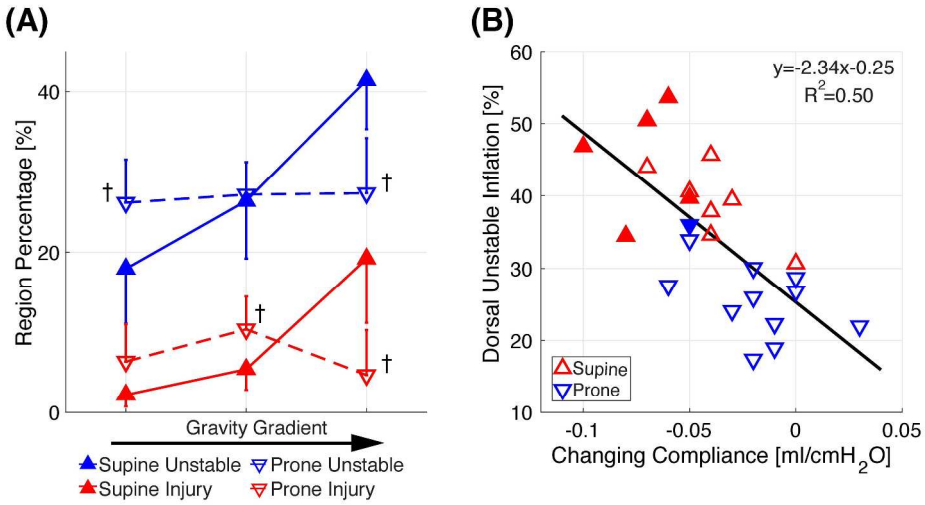

Figure 6. (A) Unstable inflation and severely injured voxels are shown (as a percent of total) in the non-dependent, mid-level, and dependent lung regions of the baseline images obtained in supine and prone rats. (B) Correlation between change in compliance (between baseline and the end of the experiment) and baseline percent fraction of unstable inflation voxels in the dependent lung regions. Solid dots indicate rats that died before two hours of ventilation. †: P<0.05 between cohorts.

279x361mm (300 x 300 DPI)

AJRCCM Articles in Press. Published on 08-February-2018 as 10.1164/rccm.201708-1728OC

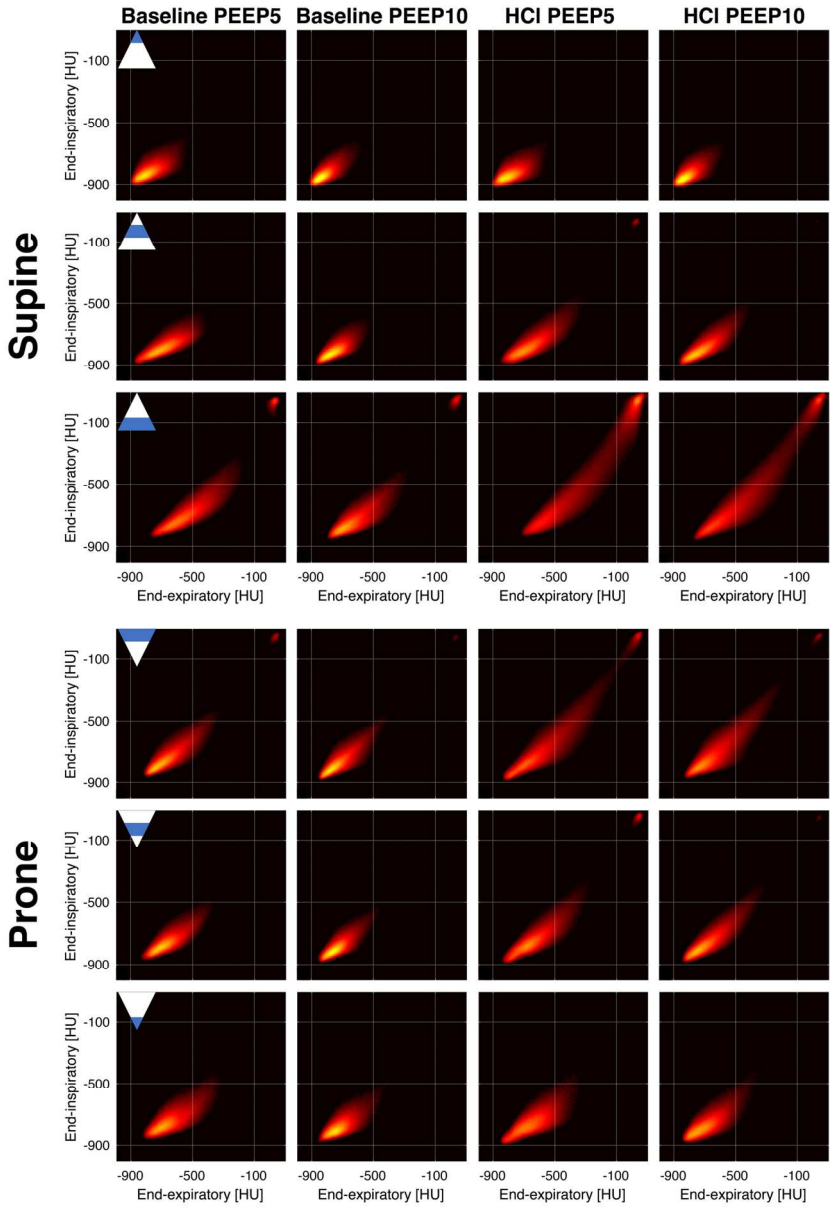

Figure 7. Cumulative parametric response maps in 5 pigs imaged before and one hour after HCl aspiration. Pigs were ventilated in the prone vs. supine position with tidal volume 8 mL·kg-1 and PEEP 5 and 10 cmH_2O. Similar to the rats, we observed a gravitational gradient of inflation distribution when the animals were supine, with more representation of unstable inflation voxels in dependent lung after injury. This maldistribution improved at higher PEEP, but it persisted in the supine position. Prone positioning caused a more homogeneous voxel distribution at both PEEP levels.

381x554mm (100 x 100 DPI)

AJRCCM Articles in Press. Published on 08-February-2018 as 10.1164/rccm.201708-1728OC

Unstable Inflation Causing Injury: Insight from Prone Position and Paired CT Scans

Yi Xin, Maurizio Cereda, Hooman Hamedani, Mehrdad Pourfathi, Sarmad Siddiqui, Natalie Meeder, Stephen Kadlecek, Ian Duncan, Harrilla Profka, Jennia Rajaei, Nicholas J. Tustison, James C. Gee, Brian P. Kavanagh, Rahim R. Rizi

Online Data Supplement

AJRCCM Articles in Press. Published on 08-February-2018 as 10.1164/rccm.201708-1728OC

Detailed Methods

All animal studies were approved by the Institutional Animal Care and Use Committee of the University of Pennsylvania (Philadelphia, PA).

Small Animals: 24 male Sprague-Dawley rats (365.3±20.9 g) were used. General anesthesia was induced and maintained with intraperitoneal pentobarbital (40–60 $mg \cdot kg^{-1}$ initially, 10–20 $mg \cdot kg^{-1} \cdot h^{-1}$ for maintenance), the trachea was intubated with a 14-gauge catheter, and the glottis was sealed to prevent gas leakage. Paralysis was obtained using pancuronium bromide (1 $mg \cdot kg^{-1}$, IV). The carotid artery was catheterized (24 gauge) for arterial blood pressure monitoring and blood gas measurement. Heart rate and oxygen saturation (SpO_2) were monitored by a veterinary pulse-oximeter (Nonin Medical, Inc. Plymouth, MN) attached to the hind foot. All animals received subcutaneous (30 mL/kg) hydration with normal saline; intravenous saline (10 $mL \cdot kg^{-1}$) was administered (three doses, maximum) if mean arterial blood pressure dropped below 40 mmHg. A rectal probe was used to monitor body temperature, which was targeted to 37 °C using a water-based heated pad.

Mechanical Ventilation: Rats were ventilated with tidal volume (V_T; 6 $mL \cdot kg^{-1}$), and positive end-expiratory pressure (PEEP; 10 cmH_2O) using a custom built small animal ventilator[1]. Airway pressure was continuously recorded using a fiber-optic sensor (Samba Sensors AB, Sweden); peak inspiratory airway pressure (PIP) and PEEP were continuously recorded, and dynamic compliance calculated: $C_{dyn} = V_T/[PIP-PEEP]$.

Lung Injury: Primary lung injury was induced by sequentially injecting 2.5 $mL \cdot kg^{-1}$ hydrochloric acid (HCl, pH 1.25) through the endotracheal tube in two aliquots, first in the right and then the left lateral position, each at 45° head elevation[2,3]. After return to the supine position, rats were stabilized for one hour with mechanical ventilation (V_T 6 $mL \cdot kg^{-1}$, PEEP 10 cmH_2O). After stabilization, rats were randomized to ventilation in the supine or prone position (12 rats in each group) for up to 3 hours, with ventilator settings known to induce secondary ventilator-induced injury[3]: V_T 12 $mL \cdot kg^{-1}$, PEEP 3 cmH_2O, FiO_2 1.0, and frequency 53 min^{-1}.

CT Imaging: High-resolution whole lung computed tomography (CT) was performed at baseline (after HCl and stabilization), as well as at each hour thereafter, using a commercial microCT scanner (eXplore CT120 system, Trifoil Imaging, Inc., Chatsworth, CA). The settings were: 80 kVp,

32 mA, 16 mS exposure time, 220 projections (half-scan), and reconstruction to 200 µm isotropic resolution. Imaging was ventilator-gated and performed during 500 mS breath-holds at both end-inspiration (EI) and end-expiration (EE). A single view was acquired during each breath-hold. In the prone group, additional sets of EI and EE images were obtained at baseline in the supine position for between-group comparisons of the severity of the primary lung injury.

Large Animals: 5 Yorkshire pigs (32.4±2.7 kg) were anesthetized with intramuscular injection of ketamine (20–25 $mg \cdot kg^{-1}$) and xylazine (2 $mg \cdot kg^{-1}$); anesthesia was maintained by continuous intravenous infusion of ketamine (7–11 $mg \cdot kg^{-1} \cdot h^{-1}$) and midazolam (0.2–0.7 $mg \cdot kg^{-1} \cdot h^{-1}$) through a peripheral catheter. The femoral artery was catheterized for blood pressure and arterial blood gas monitoring. Pigs were intubated with a 6.5 mm cuffed endotracheal tube (Teleflex Medical–Rusch, Research Triangle Park, NC, USA). SpO_2, heart rate, blood pressure (Phillips North America, Andover, MA, USA), and body temperature were monitored. All animals received intravenous hydration with normal saline (10 $mg \cdot kg^{-1}$ bolus and 1 $mg \cdot kg^{-1} \cdot h^{-1}$ infusion).

Mechanical Ventilation and Lung Injury: Animals were ventilated using a custom-made mechanical ventilator with tidal volumes of 8 $ml \cdot kg^{-1}$, frequency 15 min^{-1}, and FiO_2 0.5. All pigs were ventilated with PEEP 5 and 10 cmH_2O in both the supine and prone positions, sequentially applied in random order for periods of 10 minutes each. Imaging was performed at the end of each period. Pigs then received 2 $mL \cdot kg^{-1}$ HCl (pH 1.25) injected through the endotracheal tube in two divided doses, with the animals in the right and then left lateral position. Pigs were then stabilized supine for 30 minutes with PEEP 10 cmH_2O. After stabilization, imaging was repeated with PEEP levels and positioning as described above. Blood gases were obtained after each image acquisition.

CT Imaging: CT scans were acquired with a Siemens SOMATOM Force scanner (Siemens Medical Systems, Erlangen, Germany). EI and EE images were obtained during 5 second long inspiratory and expiratory pauses. The settings were: 120 kVp, 200 mAs, pitch 0.95, slice thickness 0.75 mm, collimation 57.6x0.6 mm, estimated dosage 3–5 mSv. All images were reconstructed to a resolution of 1x1x1 mm with QR44 kernel.

AJRCCM Articles in Press. Published on 08-February-2018 as 10.1164/rccm.201708-1728OC

Image Analysis: Image processing followed the same methodology for both small and large animals.

Image Segmentation: Lung outlines were manually delineated in baseline images (PEEP 10 cmH_2O before HCl for pigs) by trained operators using ITK-SNAP[4]. At the follow-up time points, the lung boundaries were semi-automatically segmented using a previously developed algorithm[5] to yield whole-lung 'Regions of Interest' (ROI).

Image Registration: EI and EE images were registered (aligned) to each other. The registration pipeline has been described in detail in our previous work[3]. In short, a two-step registration was used: rigid alignment by matching the bone structures (ribcage and spine) was followed by deformable registration using the symmetric diffeomorphic transformation model with B-spline regularization[6–8]. Normalized cross correlation was enforced as the similarity metric between reference and target images. This process aligned images while assuring that anatomical landmarks were in matching positions in EI and EE images[3]. This detailed reconstruction is helpful in the presence of tidal lung deformation. Each 'EI-EE' pair of images was registered for all the time points and experimental conditions. The quality of the registration has been previously validated by comparing the coordinates of major anatomical landmarks in both rats and humans[3].

Parametric Response Maps: Following registration and segmentation, parametric response maps (PRMs) were generated by matching individual voxels in each set of paired EI and EE images[9]. This methodology enables analysis of inflation distribution[9], longitudinal follow-up of lung injury progression, and quantification of progression risk. We therefore categorized all lung tissue voxels in the PRM as 'normal', 'severely injured' or 'unstable inflation', using the ranges of EI-EE density that were identified in our previous work[3]. 'Severe injury' voxels had density >-300 HU in both EI and EE images, indicating severe loss of aeration due to consolidation and unrecruitable atelectasis. Voxels with 'unstable inflation' were included in a density range (EI [-300 -700], EE [0 -500]) which was characterized by low aeration and large tidal change in density values. In our previous study[3], we longitudinally followed voxel densities and found that 'unstable inflation' voxels had the highest probability of progressing to the 'severe injury' range over time. All remaining voxels were categorized as 'normal'. We averaged the values for all

animals in each group and in each condition, and normalized them by the overall frequency distribution of the whole population. These averages allowed us to generate cumulative PRM maps. To assess the effect of gravity and position on regional inflation (and on progression of lung injury) according to the gravitational vector, lungs were partitioned into three coronal bins of equal thickness (ventral, middle and dorsal). PRM analysis was performed for the whole lung, as well as for each bin.

CT densitometry: The segmented ROIs were analyzed using standard CT densitometry[10]. Lung gas volumes were quantified with following equation:

- $\text{Gas Volume}_{ROI} = \text{Total Volume}_{ROI} \times \text{Mean CT Intensity}_{ROI}/-1000$

Where the $\text{Total Volume}_{ROI}$ included both gas and tissue volumes, and mean $\text{CT Intensity}_{ROI}$ denoted the mean value of the lung density in Hounsfield Units (HU).

Lung weight was calculated at each time point using the following equation:

- $\text{Lung Weight}_{ROI} = \text{Total Volume}_{ROI} \times (-1000-\text{Mean CT Intensity}_{ROI})/-1000.$

Thoracic geometry: To quantify the effect of prone vs. supine position on chest wall geometry, we measured the maximal height and width of lungs in the axial plane, as previously described by Valenza et al[11]. These measurements were performed using ITK-SNAP software (University of Pennsylvania, Philadelphia, PA, USA) in the 12 rats assigned to the prone group, which had both supine and prone images at baseline. The results of this analysis are reported in Table E2.

Statistical Analysis: Image analysis was performed using Matlab 2016b software (Mathworks, Natick, MA, USA) applications developed in the authors' laboratory. Statistical analysis was performed using 'R' (R Foundation for Statistical Computing, Vienna, Austria, http://www.R-project.org). Group mean and standard deviation of all the computed quantities were calculated. *Post hoc t*-tests were used to identify differences among means, and Bonferroni adjustment was performed. The Fisher exact test was used for proportions. $P<0.05$ was considered statistically significant.

AJRCCM Articles in Press. Published on 08-February-2018 as 10.1164/rccm.201708-1728OC

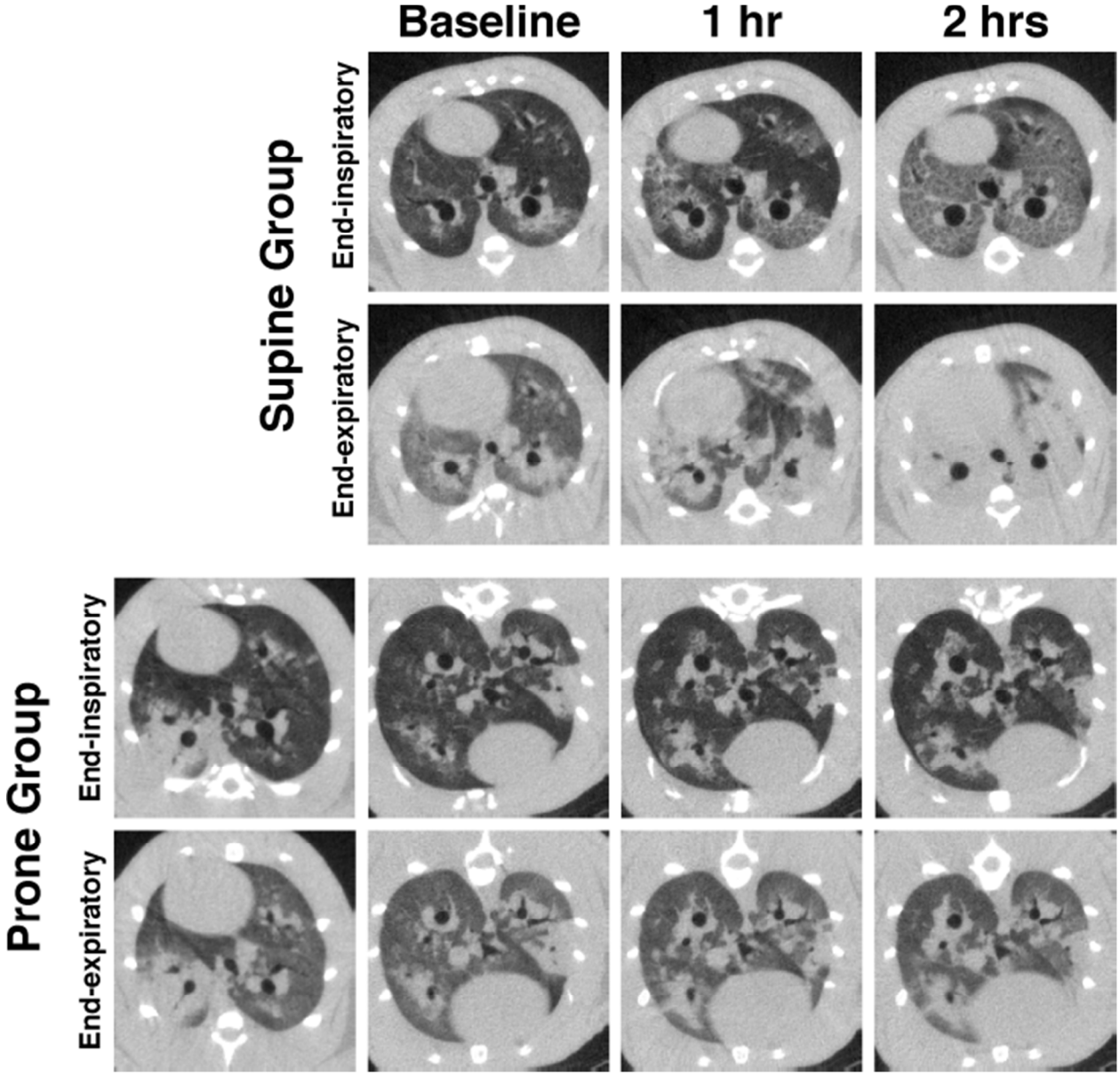

Figure E1. End-inspiratory and end-expiratory images obtained at baseline (after HCl) as well as after one and two hours of ventilation in two representative rats from the supine and prone groups. The prone rat had both supine and prone images at baseline to facilitate inter-group comparison of density distributions. The images exemplify both the effects of inflation and injury propagation in the two groups.

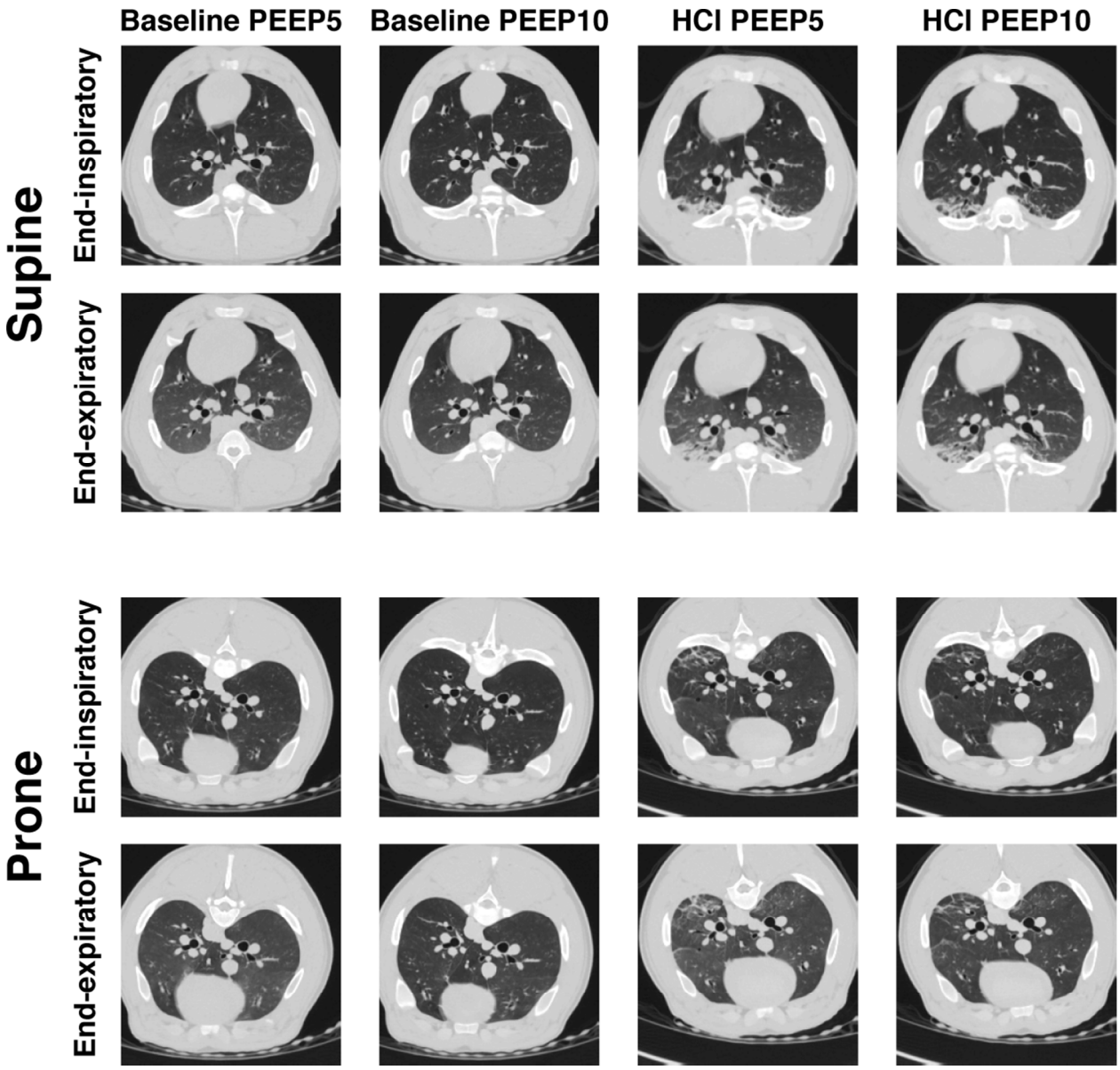

Figure E2. Representative CT images of a pig, obtained before (Baseline) and after tracheal HCl injection. Pigs were imaged at both end-inspiration (EI) and end-expiration (EE) before and after HCl, while ventilated prone and supine with two levels of PEEP (5 and 10 cmH_2O). Dorsal hyperdensities were visible after HCl in the supine position, and improved with higher PEEP. Prone position improved dorsal aeration, but its effect was more dramatic when used in combination with PEEP 10 cmH_2O.

AJRCCM Articles in Press. Published on 08-February-2018 as 10.1164/rccm.201708-1728OC

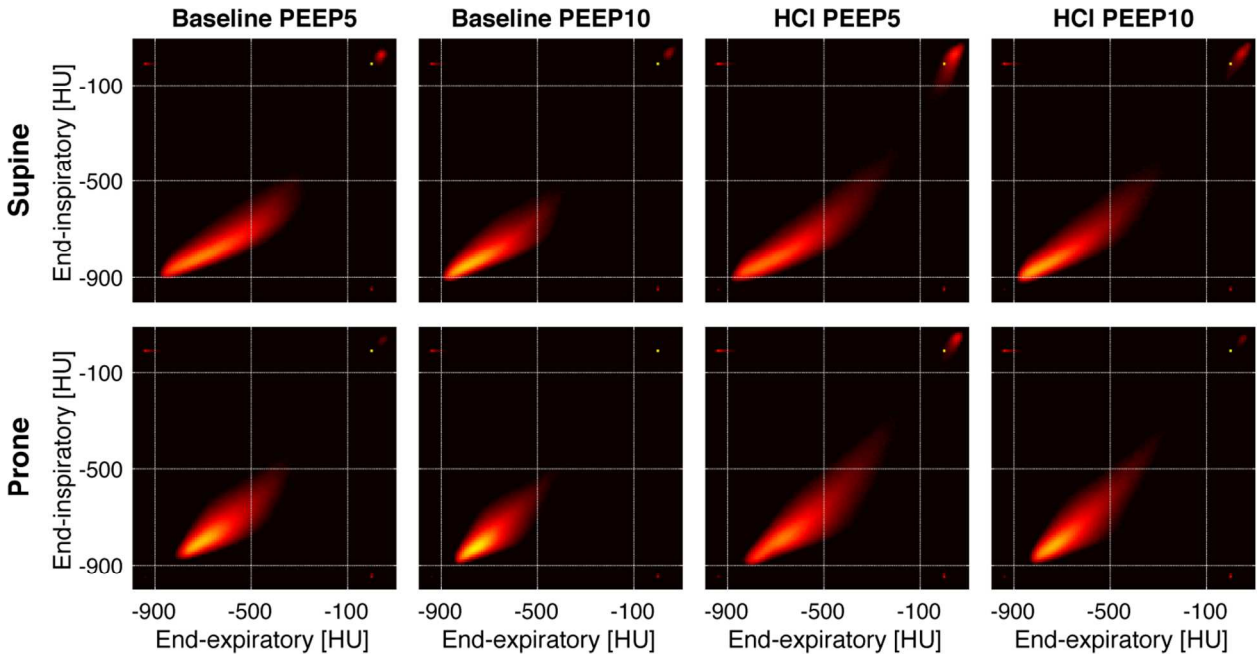

Figure E3. Cumulative whole-lung PRM obtained in 5 pigs in the same conditions as in Figure E2. The density values obtained in each condition were averaged for all pigs and normalized by the overall frequency distribution of the whole population. After HCl, prone position resulted in a narrower density distribution compared to prone. This effect was particularly evident when comparing prone position at PEEP 10 cmH_2O vs. supine position at PEEP 5 cmH_2O.

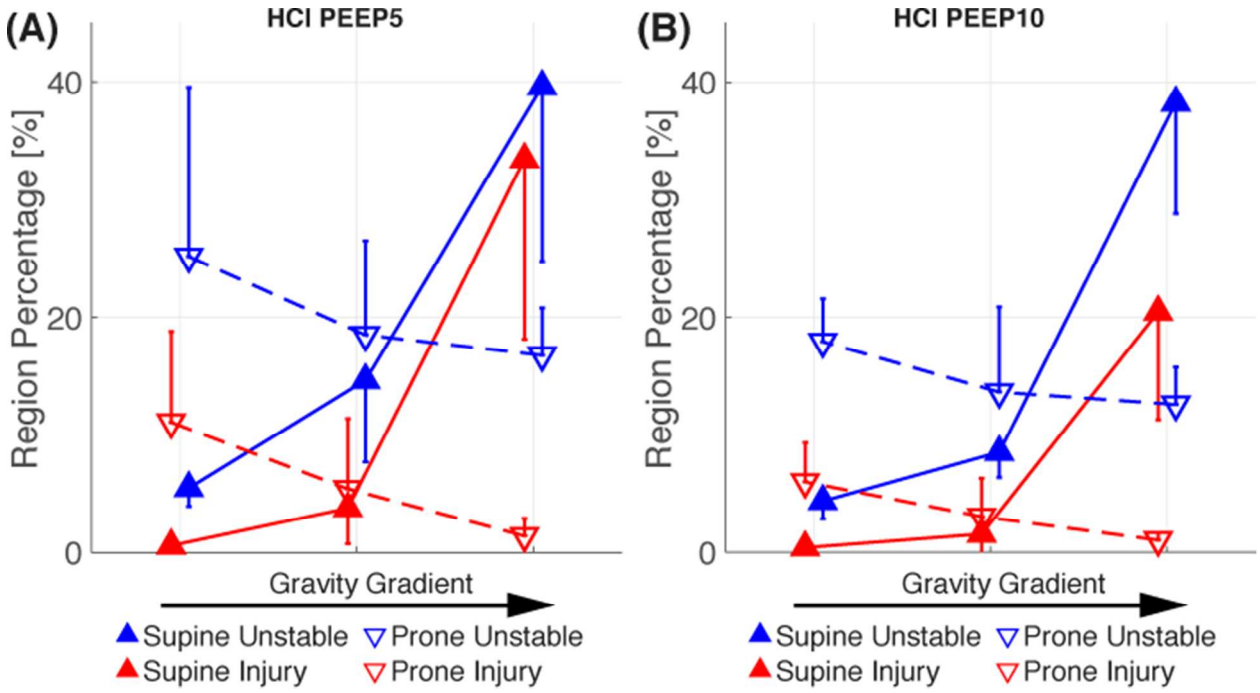

Figure E4. 'Unstable inflation' and 'severely injured' voxels are shown (as a percent of total) in the non-dependent, mid-level, and dependent lung regions of the images obtained in supine and prone pigs at two different levels of PEEP. Higher PEEP decreased the amount of severe injury voxels in all the conditions. Prone position further reduced the regional percentage of severe injury and unstable voxels. Significant vertical gradients of inflation distribution were found in the supine position, but were largely diminished in the prone position.

AJRCCM Articles in Press. Published on 08-February-2018 as 10.1164/rccm.201708-1728OC

	Baseline				HCl			
	Supine		Prone		Supine		Prone	
	PEEP 5	PEEP 10	PEEP 5	PEEP 10	PEEP 5	PEEP 10	PEEP 5	PEEP 10
Driving Pressure	13.0±2.6	16.0±1.7	12.5±2.7	14.0±1.7	19.0±4.8 §	19.8±3.4	17.8±4.6 §	17.5±2.9
pO_2	251.5±50.4	265.6±64.7	286.1±43.34	276.0±59.5	161.1±116.9 §	171.8±100.2 §	223.7±30.7 †	248.3±40.1 †
pCO_2	47.8±4.9	56.8±12.2	54.1±8.2	56.9±13.8	53.3±10.5	56.5±11.4	53.0±9.9	50.9±4.9
cSO_2	99.8±0.2	99.0±0.9	99.9±0.3	99.6±0.7	87.1±15.9 §	94.2±6.6	99.5±0.5	99.6±0.4
Blood Lactate	1.85±1.28	1.73±1.56	2.71±1.23	1.78±1.45	1.90±0.87	2.33±1.55	2.07±1.23	2.55±1.30

Table E1. Physiological characteristics of pigs ventilated in the prone vs. supine position at two different level of PEEP before and after hydrochloric acid instillation in the trachea. †: $P<0.05$ between levels of PEEP; §: $P<0.05$ supine vs. prone.

	Supine (mm)		Prone (mm)	
	height	**width**	**height**	**width**
End-inspiratory	26.44±0.85	30.46±1.12	27.74±1.47	32.12±1.11
End-expiratory	25.012±0.79	29.33±1.04	26.10±1.06	30.46±0.97

Table E2. Chest geometry (maximum height and width) of 12 rats in prone group, with both supine and prone baseline images. The chest cavity was wider in the prone position, although the differences were relatively small.

AJRCCM Articles in Press. Published on 08-February-2018 as 10.1164/rccm.201708-1728OC

ARDS	Acute respiratory distress syndrome
CT	Computed tomography
HU	Hounsfield units
EI	End-inspiratory
EE	End-expiratory
Severe injury	Lung tissue with irreversibly low gas content (i.e. density > -300 HU)
Unstable inflation	Lung tissue with elevated changes in EI/EE gas content and with high risk of worsening injury (i.e. increasing density) at later times
PRM	Parametric response map
V_T	Tidal volume
PEEP	Positive end-expiratory pressure
C_{dyn}	Dynamic compliance
PIP	Peak inspiratory pressure

Table E3. List of relevant terms and abbreviations.

REFERENCE

1. Cereda M, Emami K, Xin Y, Kadlecek S, Kuzma NN, Mongkolwisetwara P, Profka H, Pickup S, Ishii M, Kavanagh BP, Deutschman CS, Rizi RR: Imaging the Interaction of Atelectasis and Overdistension in Surfactant-Depleted Lungs*: Crit Care Med 2013; 41:527–35
2. Cereda M, Xin Y, Meeder N, Zeng J, Jiang Y, Hamedani H, Profka H, Kadlecek S, Clapp J, Deshpande CG, others: Visualizing the Propagation of Acute Lung Injury. J Am Soc Anesthesiol 2016; 124:121–131
3. Cereda M, Xin Y, Hamedani H, Bellani G, Kadlecek S, Clapp J, Guerra L, Meeder N, Rajaei J, Tustison NJ, Gee JC, Kavanagh BP, Rizi RR: Tidal changes on CT and progression of ARDS. Thorax 2017:thoraxjnl-2016-209833 doi:10.1136/thoraxjnl-2016-209833
4. Yushkevich PA, Piven J, Hazlett HC, Smith RG, Ho S, Gee JC, Gerig G: User-guided 3D active contour segmentation of anatomical structures: significantly improved efficiency and reliability. NeuroImage 2006; 31:1116–28
5. Xin Y, Song G, Cereda M, Kadlecek S, Hamedani H, Jiang Y, Rajaei J, Clapp J, Profka H, Meeder N, Wu J, Tustison NJ, Gee JC, Rizi RR: Semiautomatic segmentation of longitudinal computed tomography images in a rat model of lung injury by surfactant depletion. J Appl Physiol 2015; 118:377–85
6. Avants B, Epstein C, Grossman M, Gee J: Symmetric diffeomorphic image registration with cross-correlation: Evaluating automated labeling of elderly and neurodegenerative brain. Med Image Anal 2008; 12:26–41
7. Song G, Tustison N, Avants B, Gee JC: Lung CT image registration using diffeomorphic transformation models. Med Image Anal Clin Gd Chall 2010:23–32
8. Tustison NJ, Avants BB: Explicit B-spline regularization in diffeomorphic image registration. Front Neuroinformatics 2013; 7
9. Galbán CJ, Han MK, Boes JL, Chughtai KA, Meyer CR, Johnson TD, Galbán S, Rehemtulla A, Kazerooni EA, Martinez FJ, Ross BD: Computed tomography–based biomarker provides unique signature for diagnosis of COPD phenotypes and disease progression. Nat Med 2012; 18:1711–5
10. Caironi P, Carlesso E, Gattinoni L: Radiological imaging in acute lung injury and acute respiratory distress syndrome. Semin Respir Crit Care Med 2006; 27:404–15
11. Valenza F, Guglielmi M, Maffioletti M, Tedesco C, Maccagni P, Fossali T, Aletti G, Porro GA, Irace M, Carlesso E, Carboni N, Lazzerini M, Gattinoni L: Prone position delays the progression of ventilator-induced lung injury in rats: Does lung strain distribution play a role?*: Crit Care Med 2005; 33:361–7